



# Longitudinal dispersion coefficients in natural channels

Seyed M. Kashefipour<sup>a</sup>, Roger A. Falconer<sup>b,\*</sup>

<sup>a</sup> *Cardiff School of Engineering, Cardiff University, Water Management Research Group, P.O. Box 686, Cardiff CF24 3TB, UK*

<sup>b</sup> *Environmental Water Management, Cardiff School of Engineering, Cardiff University, Water Management Research Group, P.O. Box 686, Cardiff, Wales CF24 3TB, UK*

Received 3 November 2000; received in revised form 7 June 2001; accepted 16 July 2001

## Abstract

Details are given herein, of the development of an equation for predicting the longitudinal dispersion coefficient in riverine flows, based on 81 sets of measured data, and obtained from 30 rivers in the USA. This equation relates the dispersion coefficient to the hydraulic and geometric parameters of the flow and has been derived using dimensional and regression analysis, with a high correlation coefficient (i.e.  $R^2 = 0.84$ ). The formulation has been compared with many other existing empirical equations, frequently used to predict the longitudinal dispersion coefficient in riverine flows, with the comparisons based on four different statistical methods. These statistical comparisons have shown that the new equation appears to be more accurate than the other equations considered. The new dispersion equation was then linearly combined with a similar equation recently proposed by Seo and Cheong (J. Hydraul. Eng. ASCE 124 (1998) 25) and this combined equation was then also analysed using statistical methods. The existing empirical equations used to estimate the longitudinal dispersion coefficient and the new equations proposed in this study were included in the advective dispersion equation to predict the suspended sediment concentrations at three sites in the Humber Estuary sited along the northeast coast of England. The average percentage errors between the predicted- and measured-field data for the proposed new dispersion equations were less than those obtained using the previously documented equations. © 2002 Elsevier Science Ltd. All rights reserved.

**Keywords:** Dispersion; River mechanics; Sediment transport; Water quality; Modelling; Estuaries

## 1. Introduction

The prediction of water quality and sediment-transport fluxes in natural rivers and channels requires the solution of the mass-transport equation. Due to the nature of flow in rivers, the prevailing velocity can generally be accurately obtained by solving the one-dimensional equations of motion. Hence, the emphasis in this study has been to focus on transport in a one-dimensional framework. For unsteady non-uniform flow, the one-dimensional advective dispersion equation (ADE) is widely used to predict water quality indicator and/or suspended sediment-concentration distributions in rivers and channels, with the general form of this

equation being given as [1]

$$\frac{\partial CA}{\partial t} + \frac{\partial CAU}{\partial x} = \frac{\partial}{\partial x} AD_1 \frac{\partial C}{\partial x} + S_T, \quad (1)$$

where  $A$  is the cross-sectional area of flow,  $C$  the cross-sectional average concentration,  $U$  the cross-sectional average velocity,  $t$  the time,  $x$  the direction of mean flow velocity,  $D_1$  the longitudinal dispersion coefficient and  $S_T$  the source term.

The two main transport processes in Eq. (1), include the mean advection and dispersion. In the early stages of the transport process after an effluent has been discharged into a river, the advective term due to the turbulent velocity fluctuations plays an important role in the diffusion process. As a result, there is an imbalance between these two terms and consequently, Taylor's analysis in flow dispersion cannot be used in this section

\*Corresponding author. Fax: +44-1274-305340.

E-mail address: falconerra@cardiff.ac.uk (R.A. Falconer).

Nomenclature		RMS	root mean square
$A$	cross-sectional area	$S$	slope of energy line
$C$	cross-sectional average concentration	$S_f$	shape factor
$C_m$	cross-sectional average-measured suspended sediment concentration	$t$	time
$C_p$	cross-sectional average-predicted suspended sediment concentration	$U$	cross-sectional average velocity
DR	discrepancy ratio	$U'$	spatial deviation of velocity from cross-sectional mean velocity
$D_l$	longitudinal dispersion coefficient	$U_*$	shear velocity
$D_{lm}$	measured longitudinal dispersion coefficient	$W$	width of the channel
$D_{lp}$	predicted longitudinal dispersion coefficient	$x$	direction of mean flow
$E$	average percentage error	$y$	cartesian co-ordinate in the direction of transverse flow
$F_n$	Froude number	$\Phi$	numerical parameter for longitudinal dispersion coefficient
$H$	depth of flow	$\alpha$	ratio of $D_{lm}$ to $D_{lp}$
$l$	distance from maximum velocity to the most distant bank	$\varepsilon_y$	lateral turbulent mixing coefficient in $y$ direction
ME	mean absolute error	$\kappa$	von Karman's constant (0.41)
$N$	number of data values	$\nu$	kinematic viscosity.
$Q$	discharge		

of the flow. This imbalance leads to a skewness in the longitudinal distribution of the concentration, with the average concentration being more downstream of the originating source and with the one-dimensional dispersion equation not strictly being applicable. It is, therefore, usually assumed that the reach where the concentration of the contaminant is measured, is far enough downstream of the originating source to enable Taylor's shear flow dispersion theory to be applied [2].

In modelling these concentration distributions, the representation of the empirical coefficients, such as the longitudinal dispersion coefficient and the source terms, are critical in Eq. (1). The accuracy of the solution to the numerical scheme used to solve the ADE is highly dependent upon the accuracy of these empirical coefficients [3].

It has been established that many hydrodynamic parameters affect the longitudinal dispersion coefficient, particularly for natural rivers, where the dispersion characteristics may vary greatly from one river to another [4]. Recent laboratory observations by Guymer [5] have shown that for natural cross-sectional channel geometries, the value of the longitudinal dispersion coefficient can be as much as over 150% greater than the corresponding values obtained for regular channel cross-sections. Hence, many theoretical and empirical formulations have been proposed to determine the longitudinal dispersion coefficient ( $D_l$ ). Since many of the studies that have been undertaken to evaluate the behaviour of the dispersion coefficient have been dependent upon different assumptions in the flow conditions, the values obtained for  $D_l$  have often varied widely. In the current study, a new and simple empirical equation has

been developed for the dispersion coefficient, based upon 81 data sets collected for 30 rivers in the USA. This equation has been compared with other existing empirical equations and was also linearly combined with one of the most accurate equations published in the recent literature by Seo and Cheong [6]. The resulting combined equation was then analysed using four statistical methods and found to be highly accurate.

## 2. Previous studies

In open channel flow, Elder (1959) presented the first-published analysis of the longitudinal dispersion coefficient based on laboratory measurements and Taylor's [18] method, by assuming a logarithmic vertical-velocity distribution to give the well known equation

$$D_l = \left( \frac{0.4041}{\kappa^3} + \frac{\kappa}{6} \right) H U_* \quad \text{or} \quad D_l = 5.93 H U_*, \quad (2)$$

where  $\kappa$  is the von Karman constant, which is approximately equal to 0.41;  $U_*$  is the bed shear-stress velocity and  $H$  the depth of flow. However, it has been found that Elder's equation does not accurately describe longitudinal dispersion in natural streams and channels, and generally, significantly underestimates the dispersion coefficient. This is thought to be mainly due to the exclusion of the transverse variation in the velocity profile across the stream in the derivation of Elder's equation. Guymer and West [7] confirmed the importance of both vertical and transverse shear components of the longitudinal dispersion coefficient, according to the measurements of velocity and salinity distributions

on a cross-section in the Conwy estuary. Studies undertaken using many measured data sets for natural rivers have shown that the value of  $D_1/HU_*$  may vary from 8.6 to 7500, with values generally being much greater than Elder's equation constant of 5.93 [2].

In applying Taylor's assumptions to the mass-conservation equation for turbulent flow, and assuming that transverse or lateral variations are more important, in comparison to the vertical variations in the velocity profile, Fischer [4] presented a new equation for  $D_1$ . This equation was based on integrating the time-independent portion of the resultant conservation of mass equation over the depth and including the boundary condition of no mass flux across the bed and water surface. The resulting equation was of the following form:

$$D_1 = -\frac{1}{A} \int_0^W U'(y) H(y) \int_0^y \frac{1}{\varepsilon_y H(y)} \int_0^y U'(y) H(y) dy dy dy, \quad (3)$$

where  $U'$  is the spatial deviation of the velocity from the cross-sectional mean velocity, as a function of distance in the  $y$  direction,  $W$  is the channel width,  $y$  the cartesian co-ordinate in the transverse flow direction and  $\varepsilon_y$  the lateral turbulent mixing coefficient in  $y$  direction, which has been found, by experiment, to be typically in the region of  $0.23HU_* - 0.7HU_*$ .

Investigations have shown that Eq. (3) estimates the longitudinal dispersion coefficient more accurately than the other existing empirical equations in natural channels [8]. In practice, the integrals of Eq. (3) are replaced by similar summations and thus, in using this equation, extensive dye dispersion-field data are required in the longitudinal and transverse directions of flow [8]. In estimating  $D_1$  for practical engineering studies, it has become preferable to use equations which are based on the hydraulic and geometric parameters, and which can be readily obtained from numerical models, to represent  $D_1$ . McQuivey and Keefer [9] presented such an equation, based on combining the linear one-dimensional flow and dispersion equations, to give

$$D_1 = 0.058 \frac{Q}{SW}, \quad \text{for } F_n < 0.5, \quad (4)$$

where  $Q$  is the discharge at steady base flow,  $S$  the slope of energy line, and  $F_n$  the Froude number.

Fischer [10] developed a simple method to predict the longitudinal dispersion coefficient, which is a simplified non-integral form of Eq. (3), giving

$$D_1 = \frac{0.07U'^2 l^2}{\varepsilon_y}, \quad (5)$$

where  $l$  is the distance from the point of maximum velocity to the most distant bank. From laboratory experiments, Fischer found that  $U'^2/U^2$  varied typically

from 0.17 to 0.25, with a mean value of 0.2, and  $l$  was typically equal to  $0.7W$ . By substituting these two values into Eq. (5) and setting  $\varepsilon_y = 0.6HU_*$ , he concluded that  $D_1$  could be obtained from

$$D_1 = \frac{0.011U'^2 W^2}{HU_*}. \quad (6)$$

Since 1976, several investigators have presented empirical or experimental equations for the longitudinal dispersion coefficient as a function of the hydraulic and geometric parameters, using existing measured data in rivers or laboratory results and by mostly applying dimensional and/or regression analysis. Seo and Cheong [6] and Koussis and Rodriguez-Mirasol [11] have recently published new equations for predicting the longitudinal dispersion coefficient. Seo and Cheong derived their equation using dimensional analysis and a regression analysis for the one-step Huber method using 59 data sets, measured in 26 rivers in the USA. They used 35 of these measured data sets to establish their equation and then verified it against other data sets. Their equation can be written as

$$\frac{D_1}{HU_*} = 5.915 \left( \frac{W}{H} \right)^{0.620} \left( \frac{U}{U_*} \right)^{1.428}. \quad (7)$$

Koussis and Rodriguez-Mirasol [11], using the original theory and equation proposed by Fischer [4,10,12], and applying von Karman's defect law, derived an equation of the form

$$D_1 = \Phi \frac{U_* W^2}{H}. \quad (8)$$

They proposed a value of 0.6 for  $\Phi$  and obtained this value by applying a regression analysis on 16 field data sets. They compared their model with Fischer's model (i.e. Eq. (6)) and postulated that the results obtained from their equation were much closer to the measured data.

Swamee et al. [13] have presented the most recent investigations on the longitudinal dispersion of a solute injected from an outfall source into a channel. By assuming two logarithmic and exponential equations for mass-time curve, they derived an equation for calculating solute concentrations at any point of a river in the downstream of an originating source. They defined several dispersion parameters and related those parameters to the flow properties and channel geometry using dimensional analysis.

### 3. Development of new equation

From a review of the key literature in this field, most studies relate the longitudinal dispersion coefficient to the fluid properties, hydraulic characteristics and geo-

metric parameters. Thus, it can be postulated that

$$D_1 = f(U, H, W, U_*, \nu, S_f), \quad (9)$$

where  $\nu$  is the kinematic viscosity and  $S_f$  the shape factor. To compute the direct effect of the shape factor on the longitudinal dispersion coefficient, extensive information is required regarding the bed and wall features of a river. Furthermore, the main hydraulic parameters used to estimate  $D_1$ , such as the shear velocity, are also related to the shape factor. Since the flow in natural rivers and channels is generally fully turbulent and rough, with Reynolds number effects generally being negligible, the kinematic viscosity in Eq. (9) can be ignored as a first approximation. Dimensional analysis shows that there are many different combinations of  $H$ ,  $U$ ,  $W$  and  $U_*$ , which can lead to the same dimensions as  $D_1$ . In order to establish the best relationship to estimate the longitudinal dispersion coefficient based on the hydraulic parameters, 81 data sets measured in 30 rivers in the USA were collected from published papers by Fischer [12], McQuivey and Keefer [9] and Seo and Cheong [6], and are illustrated in Table 1.

At the first stage of the regression analysis,  $D_1$  has been related separately to all of the selected hydraulic parameters. As shown in Fig. 1, the longitudinal dispersion coefficient can be directly related to the depth of water (Fig. 1a), channel width (Fig. 1b) and velocity (Fig. 1c), whereas the data points are scattered in the  $D_1$ – $U_*$  plane (Fig. 1d). The corresponding correlation coefficients ( $R^2$ ), for the relationships between  $D_1$  and  $H$ ,  $W$  and  $U$  in Figs. 1a–c are 0.43, 0.34 and 0.38, respectively. In this regression analysis, the data sets denoted by <sup>a</sup> in Table 1 were ignored, due to their strong negative effect on the correlation coefficient in all cases. For example, when the data sets were included, the correlation coefficient for  $D_1$ – $H$  dropped to 0.06. From these relationships between  $D_1$ ,  $W$ ,  $U$  and  $H$ , it would appear that the longitudinal dispersion coefficient can be related to the products  $WU$  and  $HU$ . The corresponding plots of  $D_1$  versus  $WU$  and  $D_1$  versus  $HU$  are shown in Figs. 2a and b, respectively, with these plots demonstrating relatively pronounced linear relationships between  $D_1$  and  $WU$  and  $HU$ , respectively. The correlation between the longitudinal dispersion coefficient field data in Table 1 and the dimensionless parameters  $W/H$  and  $U/U_*$  have also been analysed and extended to exhibit reasonably good linear relationships with the relative shear velocity,  $U/U_*$ , giving an  $R^2$  value of 0.31, as shown in Fig. 3.

The correlation coefficient of all the main combinations of the selected hydraulic parameters having the same dimensions as the longitudinal dispersion coefficient were considered, including multiple regression between  $HU$ ,  $WU$  and  $D_1$ . These combinations were analysed and a best fit simple equation was derived to

give

$$D_1 = 10.612HU \left( \frac{U}{U_*} \right) \quad \text{with} \quad R^2 = 0.84. \quad (10)$$

$R^2$  for this equation is 0.84 and the relationship is shown graphically in Fig. 4.

#### 4. Comparison of models with measured data

The longitudinal dispersion coefficient is generally affected by many flow properties and channel geometry parameters and varies within a large range for different sizes and types of channels (see Table 1). A large relative error ( $> 100\%$ ) may occur in predicting this parameter, especially relatively small values. Therefore, using statistical methods based on the measured and predicted values such as normalised error, i.e.  $100\% (D_{lp} - D_{lm})/D_{lm}$ , or standard error  $(1/N \sum_{i=1}^n |D_{lp} - D_{lm}|)$ , where  $D_{lp}$  and  $D_{lm}$  are the predicted and measured values of the longitudinal dispersion, would not be sensible. For this condition, it is preferable to use the logarithm of the predicted and measured values (Eqs. (11), (13) and (14)). In the current study, four different statistical methods were applied to assess the accuracy of each model in predicting the longitudinal dispersion coefficient. The predicted dispersion coefficients obtained using Eq. (10) were compared with the measured field data, as well as with other models, including those of McQuivey and Keefer [9], Fischer [10], Seo and Cheong [6], and Koussis and Rodriguez-Mirasol [11].

The statistical methods used were as follows:

1. Discrepancy ratio (DR), defined by White et al. [14] is

$$DR = \log_{(10)} \frac{D_{lp}}{D_{lm}} = \log_{(10)} D_{lp} - \log_{(10)} D_{lm}. \quad (11)$$

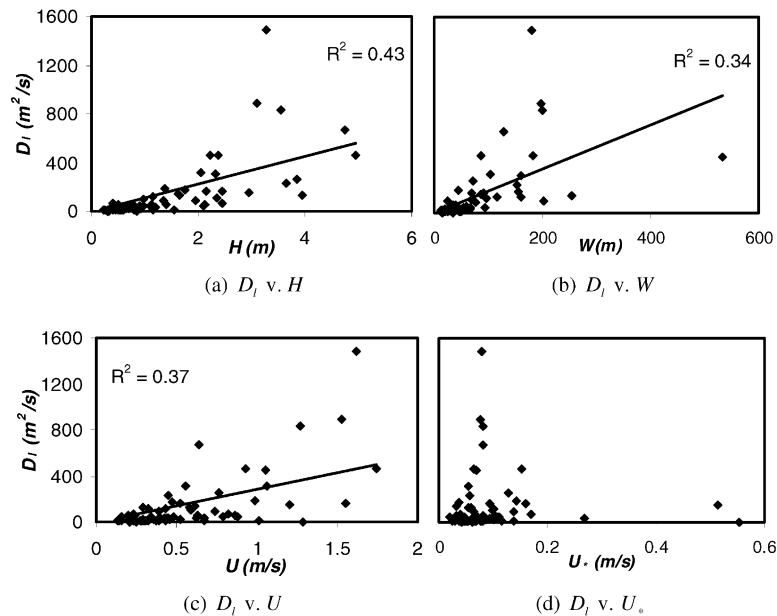
If the predicted value is equal to the measured value, then the value of DR becomes zero. For all values of DR greater than zero, the model overestimates the value of the dispersion coefficient, and conversely for values less than zero. The accuracy of each model may be categorised by the number of DR values between  $-0.3$  and  $0.3$ , relative to the total number of data values. This range was selected due to the maximum acceptable error in predicting the longitudinal dispersion coefficient from the corresponding measured values ( $\pm 100\%$ , or  $D_{lp}/D_{lm} = 0.5$ – $2.0$ ). Seo and Cheong [6] used the same range of DR values for establishing a way to assess the different formulations for the longitudinal dispersion coefficient. Moog and Jirka [15] introduced a relatively similar method to the discrepancy ratio, for assessing the predicted and measured stream re-aeration coefficient.

Table 1  
Experimental measurements of longitudinal dispersion in natural channels

Source	Channel	$H$ (m)	$W$ (m)	$U$ (m/s)	$U_*$ (m/s)	$D_L$ (m <sup>2</sup> /s)
Fischer [12]	Copper creek, VA (below gage)	0.49	15.9	0.21	0.079	19.52
		0.84	18.3	0.52	0.100	21.40
		0.49	16.2	0.25	0.079	9.50
	Clinch river, TN (below gage)	0.86	46.9	0.28	0.067	13.93
		2.13	59.4	0.86	0.104	53.88
		2.09	53.3	0.79	0.107	46.45
	Copper creek, VA (above gage)	0.39	18.6	0.14	0.116	9.85
	Power river, TN	0.85	33.8	0.16	0.055	9.50
	Clinch river, VA	0.58	36.0	0.30	0.049	8.08
	Coachell canal, CA	1.56	24.4	0.67	0.043	9.57
McQuivey and Keefer [9]	Bayou Anacoco	0.94	25.9	0.34	0.067	32.52
		0.91	36.6	0.40	0.067	39.48
		0.41	19.8	0.29	0.044	13.94
	Nooksack river	0.76	64.0	0.67	0.268	34.84
		2.94	86.0	1.20	0.514	153.29
	Antietam creek	0.39	15.8	0.32	0.060	9.29
		0.52	19.8	0.43	0.069	16.26
		0.71	24.4	0.52	0.081	25.55
	Monocacy river	0.32	35.1	0.21	0.043	4.65
		0.45	36.6	0.32	0.051	13.94
		0.87	47.5	0.44	0.070	37.16
	Missouri river	2.23	182.9	0.93	0.065	464.52
		3.56	201.2	1.27	0.082	836.13
		3.11	196.6	1.53	0.077	891.87
	Wind/Bighorn rivers	0.98	67.1	0.88	0.110	41.81
		2.16	68.6	1.55	0.161	162.58
	Elkhorn river	0.30	32.6	0.43	0.046	9.29
		0.42	50.9	0.46	0.046	20.90
	John Day river	0.56	25.0	1.01	0.137	13.94
		2.46	34.1	0.82	0.169	65.03
	Comite river	0.26	12.5	0.31	0.043	6.97
		0.41	15.8	0.37	0.055	13.94
	Amite river	0.81	36.6	0.29	0.068	23.23
		0.80	42.4	0.42	0.068	30.19
	Sabine river	2.04	103.6	0.56	0.054	315.87
		4.75	127.4	0.64	0.081	668.90
	Yadkin river	2.35	70.1	0.43	0.101	111.48
		3.84	71.6	0.76	0.128	260.13
	Muddy creek	0.81	13.4	0.37	0.077	13.94
		1.20	19.5	0.45	0.093	32.52
	Sabine river, Texas	0.98	35.1	0.21	0.041	39.48
	White river	0.55	67.1	0.35	0.044	30.19
	Chattahoochee river	1.13	65.5	0.39	0.075	32.52
	Susquehanna river	1.35	202.7	0.39	0.065	92.90
Seo and Cheong [6]	Antietam creek, MD	0.98	24.1	0.59	0.098	101.50
		0.66	11.9	0.43	0.085	20.90
	Monocacy river, MD	0.71	93.0	0.16	0.046	41.40
		0.65	51.2	0.62	0.044	29.60
		1.15	97.5	0.32	0.058	119.80
		0.41	40.5	0.23	0.040	66.50
	Conococheague creek, MD	0.69	42.2	0.23	0.064	40.80
		0.41	49.7	0.15	0.081	29.30
		1.13	43.0	0.63	0.081	53.30

Table 1 (continued)

Source	Channel	$H$ (m)	$W$ (m)	$U$ (m/s)	$U_*$ (m/s)	$D_I$ (m <sup>2</sup> /s)
	Chattahoochee river, GA	1.95	75.6	0.74	0.138	88.90
		2.44	91.9	0.52	0.094	166.90
	Salt creek, NE	0.50	32.0	0.24	0.038	52.20
	Difficult run, VA	0.31	14.5	0.25	0.062	1.90
	Bear creek, CO	0.85	13.7	1.29	0.553	2.90
	Little Pincy creek, MD	0.22	15.9	0.39	0.053	7.10
	Bayou Anacoco, LA	0.45	17.5	0.32	0.024	5.80
	Bayou Bartholomew, LA	1.40	33.4	0.20	0.031	54.70
	Amite river, LA	0.52	21.3	0.54	0.027	501.40 <sup>a</sup>
	Tickfau river, LA	0.59	14.9	0.27	0.080	10.30
	Tangipahoa river, LA	0.81	31.4	0.48	0.072	45.10
	Red river, LA	0.40	29.9	0.34	0.020	44.00
		1.62	253.6	0.61	0.032	143.80
		3.96	161.5	0.29	0.060	130.50
		3.66	152.4	0.45	0.057	227.60
	Sabine river, LA	1.74	155.1	0.47	0.036	177.70
		1.65	116.4	0.58	0.054	131.30
		2.32	160.3	1.06	0.054	308.90
	Sabine river, TX	0.50	14.2	0.13	0.037	12.80
		0.51	12.2	0.23	0.030	14.70
		0.93	21.3	0.36	0.035	24.20
	Mississippi river, LA	19.94	711.2	0.56	0.041	237.20 <sup>a</sup>
	Mississippi river, MO	4.94	533.4	1.05	0.069	457.70
		8.90	537.4	1.51	0.097	341.10 <sup>a</sup>
	Wind/Bighorn river, WY	1.37	44.2	0.99	0.142	184.60
		2.38	85.3	1.74	0.153	464.60
	Clinch river, VA	1.16	48.5	0.21	0.069	14.76
	Missouri river	3.28	180.6	1.62	0.078	1486.45

<sup>a</sup>Data sets used just for statistical analysis.Fig. 1. Relationship between  $D_I$  and (a)  $H$ , (b)  $W$ , (c)  $U$  and (d)  $U_*$ .

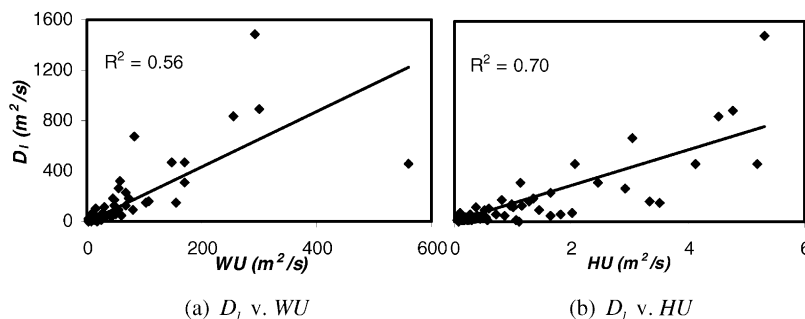


Fig. 2. Relationship between  $D_l$  and (a)  $WU$  and (b)  $HU$ .

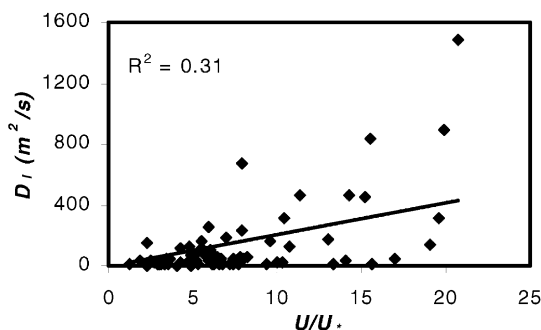


Fig. 3. Relationship between  $D_l$  and  $U/U_*$ .

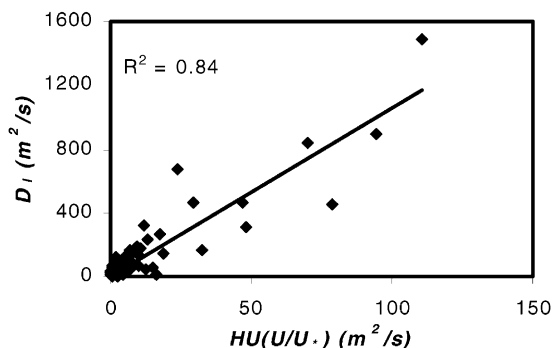


Fig. 4. Variation of  $D_l$  with  $HU(U/U_*)$ .

2.  $R^2$  and  $\alpha$ , are given by the following ratio:

$$\alpha = \frac{D_{lm}}{D_{lp}}. \quad (12)$$

It is evident that, for each model, whenever the coefficient of  $\alpha$  is close to unity and the correlation coefficient is high, this will give rise to a more accurate prediction. The least-squares method has been applied to estimate  $\alpha$  and  $R^2$  for each model and the results are summarised in Table 2.

3. The mean of the absolute error (ME) is defined by

$$ME = \frac{1}{N} \sum_{i=1}^N |DR_i|. \quad (13)$$

4. The root mean square (RMS) with this index is written as

$$RMS = \frac{1}{N} \sqrt{\sum_{i=1}^N (DR_i)^2}, \quad (14)$$

where  $N$  is the total number of data.

To obtain good model predictions, the resulting values for Eqs. (13) and (14) should be as close as possible, to zero. Therefore, the difference between the calculated values for ME and RMS and zero, can help in establishing the relative accuracy of each model in predicting the dispersion coefficient. The existing empirical equations and Eq. (10) were compared to the measured data, using the above-outlined statistical methods and the final results are summarised in Table 2.

A comparison of the results in Table 2 shows that the percentage of the observed discrepancy ratio values between  $-0.3$  and  $0.3$  is only over 50% for three models, including the models given by McQuivey and Keefer [9], Seo and Cheong [6] and Eq. (10). Further consideration of the models using Eq. (12), and the results in Table 2, shows that two of these models are preferable, namely the Seo and Cheong [6] model and Eq. (10), with the model given by Eq. (10) appearing to be more accurate according to this statistical parameter. These two later models again appeared to be preferable in predicting the longitudinal dispersion coefficient when comparing the results of the various models for ME and RMS values. In summary, the overall results from Table 2 suggest that Seo and Cheong's model and that given by Eq. (10) were the most accurate models for predicting the longitudinal dispersion coefficient  $D_l$  in natural channels. From this table, it can be seen that the equations of Fischer and Koussis and Rodriguez-Mirasol, both overestimated the longitudinal dispersion coefficients.

Table 2  
Comparison of various models using four statistical methods

Model	DR proportion (%)				Eq. (12)		ME	RMS
	<−0.3	−0.3–0	0–0.3	> 0.3	$\alpha$	$R^2$		
McQuivey and Keefer [9]	14.8	25.9	34.6	24.7	0.396	0.523	0.36	0.061
Fischer [10]	22.2	19.8	14.8	43.2	0.109	0.229	0.49	0.068
Seo and Cheong [6]	9.8	19.8	43.2	27.2	0.630	0.703	0.31	0.046
Koussis and R. Mirasol [11]	11.2	18.5	25.9	44.2	0.370	0.100	0.47	0.066
Eq. (10)	28.4	42.0	18.5	11.1	1.000	0.840	0.35	0.050
Eq. (15)	18.5	34.6	29.6	17.3	0.880	0.800	0.29	0.032

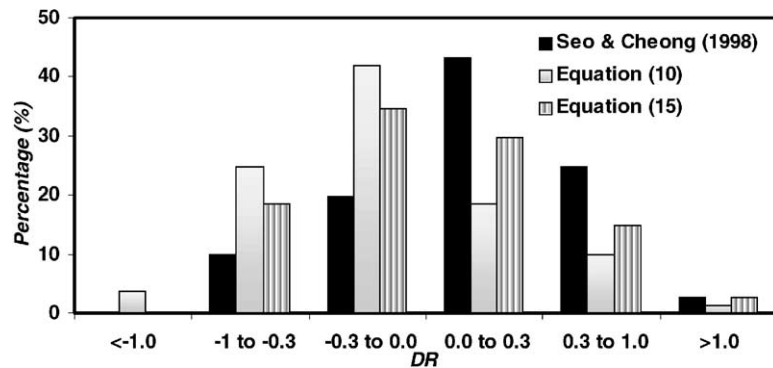


Fig. 5. Comparison of discrepancy ratio for Seo and Cheong's model, and Eqs. (10) and (15).

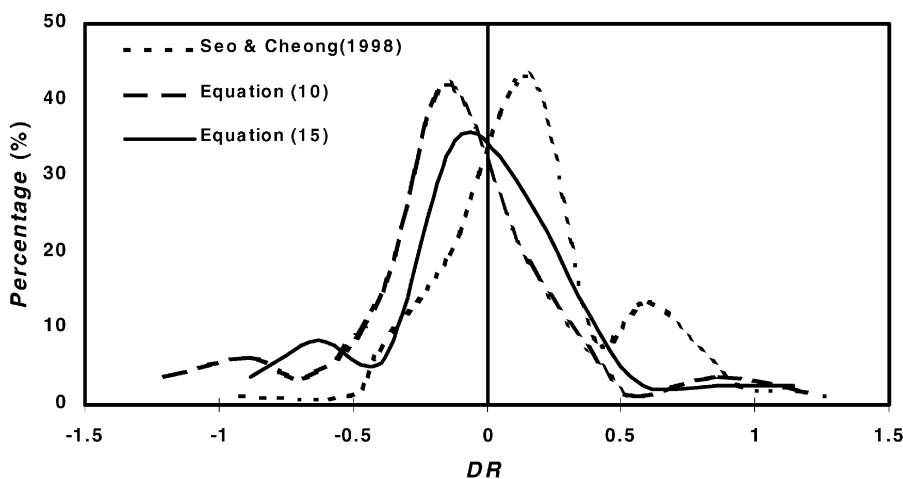


Fig. 6. Distribution of percentage of DR values for three models.

According to the results of Table 2, the percentage of discrepancy ratio values greater than zero were 70.4% for Seo and Cheong's model and 29.6% for Eq. (10). These results meant that Seo and Cheong's model generally overestimated the predicted longitudinal dispersion coefficient, whereas Eq. (10) underestimated the coefficients. These findings can also be confirmed from

Figs. 5 and 6. The skewness of the results for Seo and Cheong's model was towards the positive zone, whereas the skewness obtained using Eq. (10) was towards the negative zone. The percentage of DR values between 0.3 and 1.0, and −1.0 and −0.3 for Seo and Cheong's model were 24.7% and 9.9%, respectively, whereas the corresponding values for Eq. (10) were 9.9% and



24.7%, respectively (see Fig. 5). In addition, according to Table 1, as a comparative factor, the average computed ratio of  $D_l/HU_*$  for the Seo and Cheong equation and Eq. (10) were 1508.0 and 887.0, respectively, whereas the corresponding average measured ratio was 1045. Therefore, it seemed appropriate to combine these equations in a linear manner, to estimate the longitudinal dispersion coefficient more accurately and obtain a good lognormal distribution (see Fig. 6). By trial and error and comparison of the predicted longitudinal dispersion coefficients with the corresponding measured values, the most appropriate equation has been obtained, giving

$$D_l = \left[ 7.428 + 1.775 \left( \frac{W}{H} \right)^{0.620} \left( \frac{U_*}{U} \right)^{0.572} \right] HU \left( \frac{U}{U_*} \right). \quad (15)$$

Eq. (15) was derived by linearly combining 30% of Seo and Cheong's equation and 70% of Eq. (10). The ratio of  $D_l/HU_*$  for this equation was 1073.0, which is close to the corresponding measured ratio. A comparison of Eqs. (10) and (15) shows that the constant coefficient of 10.612 has been replaced by  $[7.428 + 1.775(W/H)^{0.620}(U_*/U)^{0.572}]$ .

The statistical results relating to Eq. (15) have been obtained and are appended in Table 2. These results suggest that Eq. (15) estimates the longitudinal dispersion coefficient more accurately than all the other equations considered. The percentage of observed DR values greater than zero is equal to 46.9% and the values in the range from  $-1.0$  to  $-0.3$  and from  $0.3$  to  $1.0$  are

18.5% and 14.8%, respectively (see Fig. 5). The accuracy of Eq. (15) in terms of the DR values being in the range from  $-0.3$  to  $0.3$  is 64.2%, which is marginally better than predictions for both Eq. (10) and Seo and Cheong's model. In Fig. 6, the percentage of data values falling within each range of the discrepancy ratio (DR) are plotted for each model, with the peak DR value of zero, being closer using Eq. (15) than for either of the other two formulations.

The measured data were plotted against the predicted data using the proposed new models (i.e. Eqs. (10) and (15)) in Figs. 7a and b. Further investigations on the predicted longitudinal dispersion coefficients using Eqs. (10) and (15) showed that for open channel flows with  $W/H$  values in excess by 50, the predicted values given using Eq. (10) were closer to the measured data than the corresponding values predicted using Eq. (15). On the contrary, the predicted values obtained using Eq. (15) for channels with  $W/H$  ratios less than 50 showed better agreement with the measured data, than those values obtained using Eq. (10). Thus, in practical applications or research studies for estimating the longitudinal dispersion coefficient, it is suggested that best predictions will be obtained by applying Eqs. (10) or (15) for open channels with  $W/H$  values greater or less than 50, respectively.

## 5. Application and evaluation of models

In considering the discussions and comparisons cited herein, the predicted  $D_l$  values obtained from either

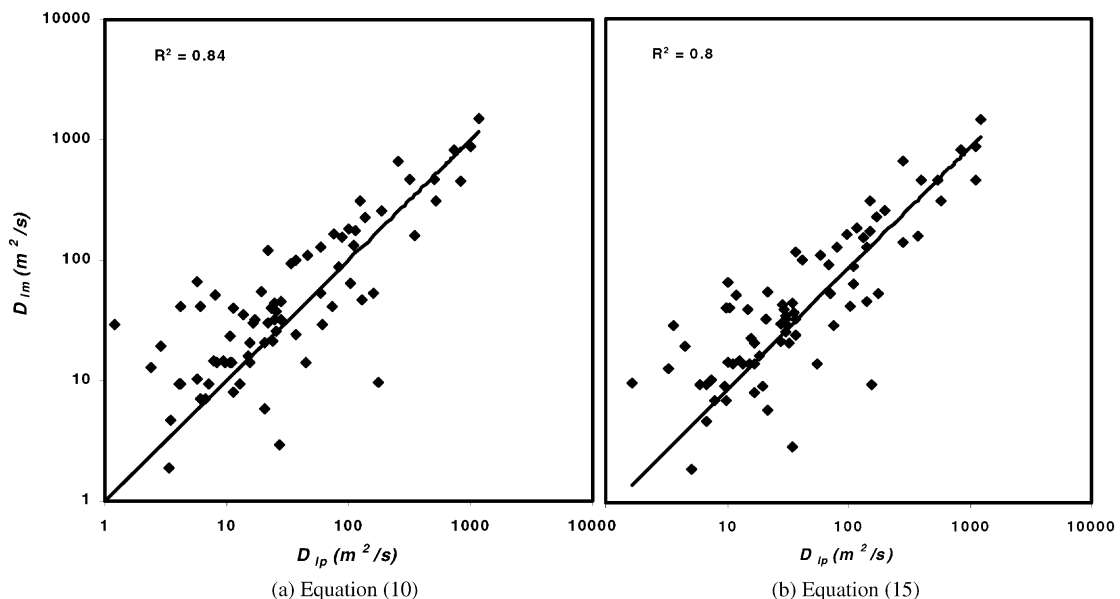


Fig. 7. Comparison of measured ( $D_{lm}$ ) and predicted ( $D_{lp}$ ) longitudinal dispersion coefficients using Eqs. (10) and (15). (a) Eq. (10), (b) Eq. (15).

Eqs. (10) or (15) were found to be more accurate than the other models considered. However, it is more practical to include all of the above mentioned formulations in the advective dispersion equation (i.e. Eq. (1)) to predict the water quality or suspended sediment-concentration distributions in the same way and then compare them with measured values in evaluating the accuracy of each model prediction.

The dispersion formulations of McQuivey and Keefer [9], Fischer [10], Seo and Cheong [6], Koussis and Mirasol [11], and from Eqs. (10) and (15), were then included in the advective diffusion equation (i.e. Eq. (1)), to predict suspended sediment-concentration distributions in the Humber Estuary and its tributaries (see Fig. 8). This estuary is a major coastal inlet sited along the northeast coast of England. It drains about 20% of England, primarily via the rivers Trent and Ouse, and discharges into the North Sea. The estuary is highly dynamic and has a typical spring tidal range of 7.0 m over its main basin, stretching 60 km from Spurn Head in the east to Trent Falls in the west. Along the estuary, extensive hydrodynamic, water-quality and suspended sediment-concentration data have been acquired for many years, and by various organisations, for a range of hydrodynamic and meteorological conditions. In parti-

cular, Associated British Ports (formerly British Transport Docks Board [16]) have taken extensive measurements of water elevations, velocities and suspended-sediment concentrations at a number of elevations through the water column at Sunk Channel, Middle Shoal and Halton Middle (Fig. 8). The downstream model considered in this application was Bull Fort and the upstream was extended up to the tidal limits of the rivers Trent, Ouse, Don, Aire and Wharfe, as shown in Fig. 8.

In predicting the suspended-sediment concentrations, the advective dispersion equation (ADE), i.e. Eq. (1), was solved using a finite volume method [17] with the water surface elevation and velocity at any point and time being obtained from the numerical solution of the Saint Venant equations. The source term in Eq. (1) was specified using a new empirical representation, which has recently been proposed for river and estuarine systems by Kashefipour and Falconer [3].

The measured and predicted suspended-sediment concentrations, obtained for spring and mid-tide conditions, at three measuring sites along the Humber Estuary were considered to assess the accuracy of the formulations for the longitudinal dispersion coefficient in terms of the prediction of the suspended-sediment

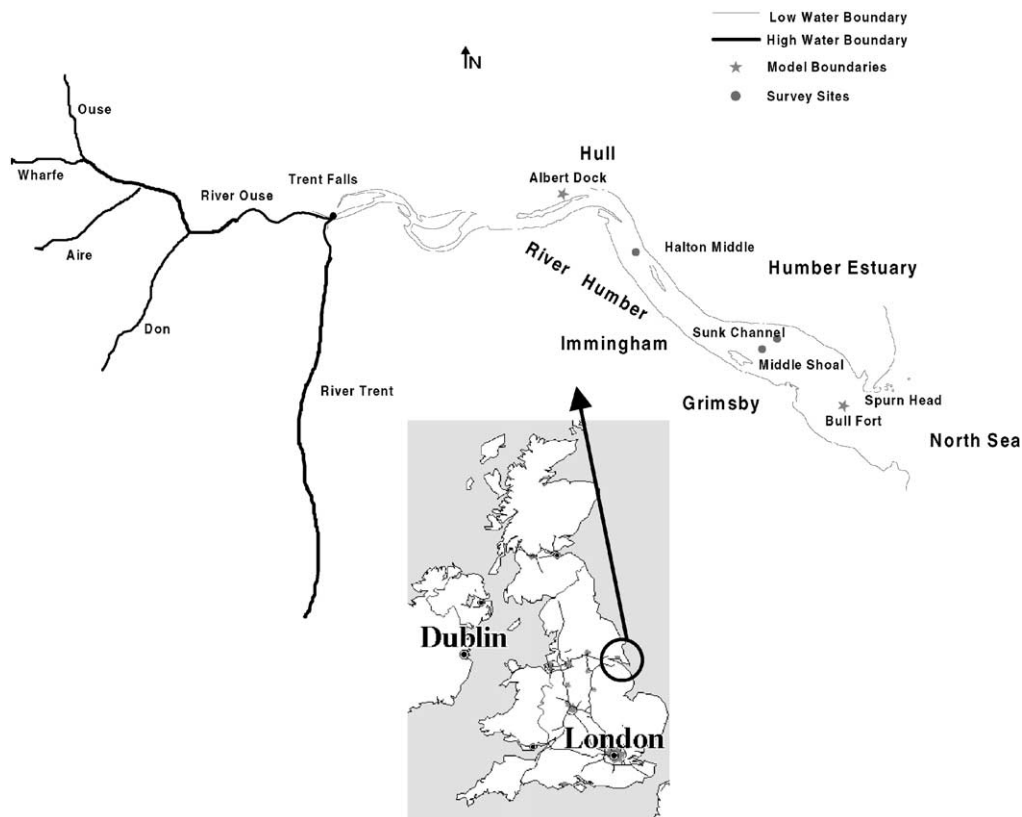
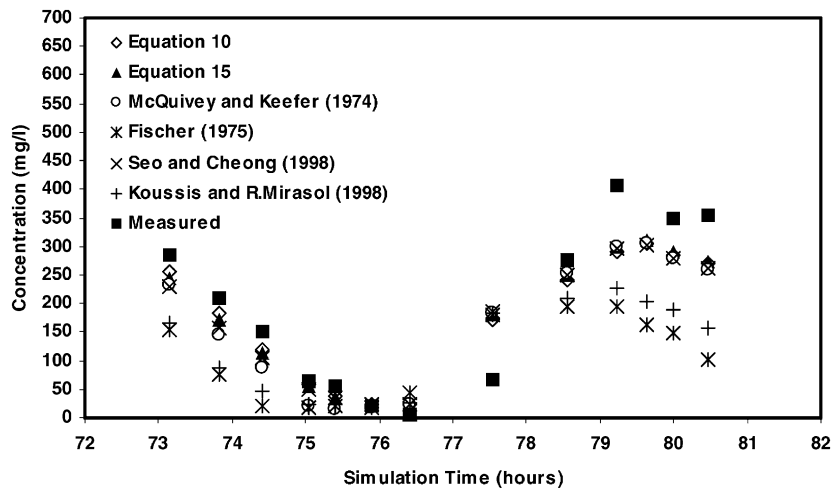
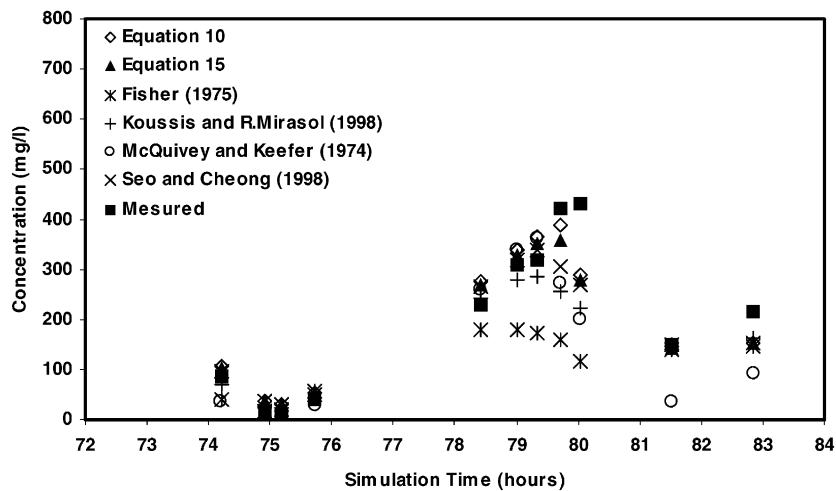


Fig. 8. Plan of Humber estuary and its tributaries.



(a) Sunk Channel-Spring Tide



(b) Halton Middle-Mid Tide

Fig. 9. Comparison of predicted and measured suspended-sediment concentrations with different dispersion formulations used in ADE. (a) Sunk channel-spring tide, (b) Halton middle-mid-tide.

concentrations. Suspended-sediment concentrations at Sunk Channel, Middle Shoal, and Halton Middle, for spring and mid-tides, were predicted using Eq. (1), in which the considered models were used to estimate the longitudinal dispersion coefficient ( $D_L$ ). Figs. 9a and b show two typical comparisons of the predicted suspended-sediment concentrations with the measured values for the spring and mid-tides at Sunk Channel and Halton Middle, respectively. As can be seen from these figures, the predicted values obtained using Eqs. (10) and (15), as applied to estimate  $D_L$ , show better agreement with the measured suspended-sediment concentrations than the other equations considered for

$D_L$ . The average percentage error in the model predictions was then evaluated using the following equation to compare, quantitatively, the accuracy of the dispersion equations considered:

$$E = \frac{\sum_{i=1}^N |C_{mi} - C_{pi}|}{\sum_{i=1}^N C_{mi}} \times 100\%, \quad (16)$$

where  $E$  is the average percentage error,  $N$  the total number of measured values and  $C_m$  and  $C_p$  are the measured and predicted concentrations, respectively.

The measured suspended-sediment concentrations at all sites and for all tides were used to calculate the average percentage error for each dispersion formula-

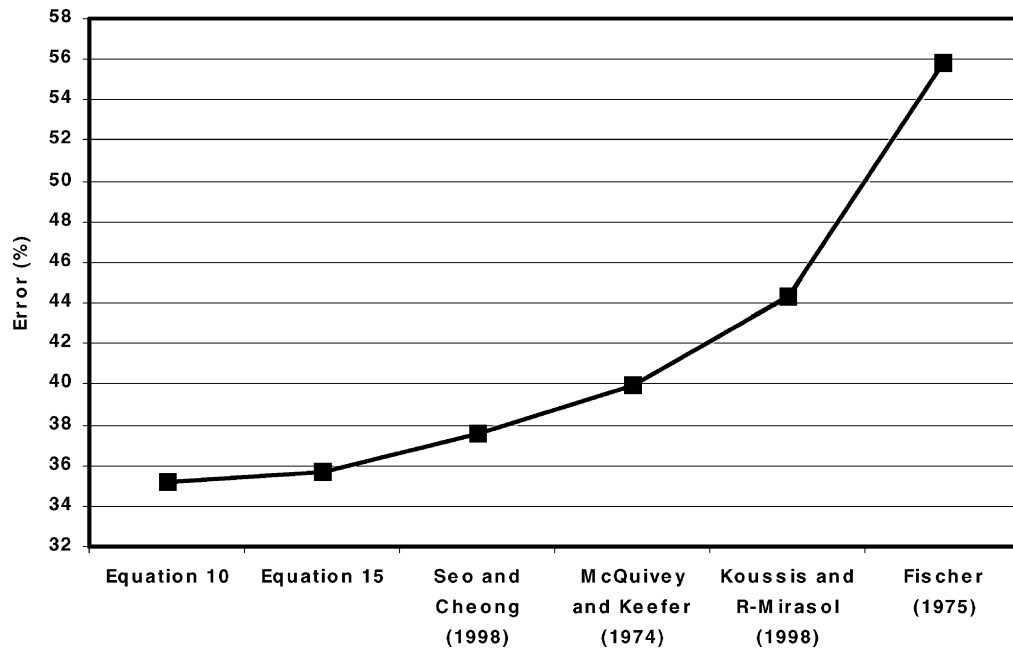


Fig. 10. Average percentage error in predicting suspended-sediment concentrations for various dispersion formulations in ADE.

tion. The minimum and maximum average percentage errors were obtained for Eq. (10) and Fischer's formulation, giving values of 35.15% and 55.78%, respectively. Fig. 10 shows the average percentage error in predicting the suspended-sediment concentrations due to the formulations applied to estimate the longitudinal dispersion coefficient ( $D_L$ ) in the advective dispersion equation (i.e. Eq. (1)). From these results, it can be seen that the errors obtained in predicting the suspended-sediment concentrations using both the proposed Eqs. (10) and (15) for estimating the longitudinal dispersion coefficient were less than the corresponding results obtained using the other formulations. Thus, in this paper, both Eqs. (10) and (15) are suggested as improved formulations to estimate the longitudinal dispersion coefficients in practical- or research-oriented hydro-environmental model studies.

## 6. Conclusions

The main conclusions from this study can be summarised as follows:

1. A new relationship has been established for predicting the longitudinal dispersion coefficient in natural channels (i.e. Eq. (10)), by relating this process through dimensional and regression analysis to the main hydraulic parameters of river depth, width, velocity and shear velocity. In developing this relationship, 81 data sets were used for 30 rivers in the USA.
2. A comparison of this new relationship with several existing equations for the dispersion coefficient, and using four statistical methods for analysis, has shown that the accuracy of this model compared favourably with other equations in the literature.
3. A comparison of the correlation coefficient and the ratio of the predicted and measured dispersion coefficients (i.e. Eq. (12)) was undertaken for the new equation (i.e. Eq. (10)), Seo and Cheong's formulation and McQuivey and Keefer's formulation, with the corresponding values being (0.84, 1.0), (0.703, 0.63) and (0.523, 0.396), respectively. These results indicate that the new equation (i.e. Eq. (10)) was more accurate than the other formulations.
4. The formulations of Seo and Cheong, McQuivey and Keefer, and Koussis and Rodriguez-Mirasol were found to estimate the measured  $D_L$  values reasonably well, whereas the predicted dispersion coefficients obtained using Fischer's formulation generally over-estimated the measured  $D_L$  values.
5. By trial and error, a linear combination of the new formulation (i.e. Eq. (10)) and Seo and Cheong's formulation led to a further new model (i.e. Eq. (15)), which when tested for the same 81 data sets, led to a further improved equation for predicting the longitudinal dispersion coefficient in riverine and channel flows.

6. Finally, all of the longitudinal dispersion coefficient formulations were included in the advective dispersion equation to predict suspended-sediment concentrations at three sites in the Humber Estuary, sited along the northeast of England, UK, for spring- and mid-tides. Comparisons of the predicted and measured concentrations again showed that the average error between both sets of results were less for the new equations proposed in the paper (i.e. Eqs. (10) and (15)), in comparison with the results obtained for the other considered published formulations.

### Acknowledgements

The first author would like to acknowledge the support of the Iranian Ministry of Culture and Higher Education (MCHE) in supporting this research project at Cardiff University.

### References

- [1] Rutherford JC, O'Sullivan MJ. Simulation of water quality in Tarawera River. *J Environ Eng Div ASCE* 1974;100:369–90.
- [2] Fischer HB, List EJ, Koh RY, Imberger J, Brooks NH. Mixing in inland and coastal waters. New York: Academic Press, 1979. 483pp.
- [3] Kashefipour SM, Falconer RA. An improved model for predicting sediment fluxes in estuarine waters. Proceedings of the Fourth International Hydroinformatics Conference, Iowa, USA, July 2000. p. 1–8.
- [4] Fischer HB. The mechanics of dispersion in natural streams. *J Hydraul Division ASCE* 1967;93:187–216.
- [5] Guymer I. Longitudinal dispersion in sinuous channel with changes in shape. *J Hydraul Eng ASCE* 1998;124:33–40.
- [6] Seo IW, Cheong TS. Predicting longitudinal dispersion coefficient in natural streams. *J Hydraul Eng ASCE* 1998;124:25–32.
- [7] Guymer I, West JR. Longitudinal dispersion coefficients in estuary. *J Hydraul Eng ASCE* 1992;118:718–34.
- [8] French RH. Open-channel hydraulics. New York: McGraw-Hill, 1985. 705pp.
- [9] McQuivey RS, Keefer TN. Simple method for predicting dispersion in streams. *J Environ Eng ASCE* 1974;100:997–1011.
- [10] Fischer HB. Discussion of 'simple method for predicting dispersion in streams' by R.S. McQuivey and T.N. Keefer. *J Environ Eng Div ASCE* 1975;101:453–5.
- [11] Koussis AD, Rodriguez-Mirasol J. Hydraulic estimation of dispersion coefficient for streams. Technical Note. *J Hydraul Eng ASCE* 1998;124:317–20.
- [12] Fischer HB. Dispersion predictions in natural streams. *J Sanit Eng ASCE* 1968;94:927–43.
- [13] Swamee PK, Pathak SK, Sohrab M. Empirical relations for longitudinal dispersion in streams. *J Hydraul Eng ASCE* 2000;126:1056–62.
- [14] White WR, Milli H, Crabbe AD. Sediment transport: an appraisal methods, vol. 2: Performance of theoretical methods when applied to flume and field data. Hydraulic Research Station Report No. IT119, Wallingford, UK, 1973.
- [15] Moog DB, Jirka GH. Analysis of reaeration equations using mean multiplicative error. *J Hydraul Eng ASCE* 1998;124:104–10.
- [16] British Transport Docks Board. Humber estuary sediment flux. Part I: Field measurements. British Transport Docks Board, Research Station Report No. 283, 1980. 91pp.
- [17] Kashefipour SM, Falconer RA. Numerical modelling of suspended sediment fluxes in open channel flows. Proceedings of the XXVIII IAHR Congress, 22–27 August 1999, Graz, Austria, 1999. p. 1–6.
- [18] Taylor GI. The dispersion of matter in turbulent flow through a pipe. *Proc R Soc London* 1954;A223: 446–68.